Biochem. J. (2011) **436**, 399–407 (Printed in Great Britain) doi:10.1042/BJ20101490

Hypoxia down-regulates sFlt-1 (sVEGFR-1) expression in human microvascular endothelial cells by a mechanism involving mRNA alternative processing

Takayuki IKEDA*[1], Li SUN*†[1], Naoki TSURUOKA*, Yasuhito ISHIGAKI‡, Yasuo YOSHITOMI*, Yoshino YOSHITAKE* and Hideto YONEKURA*[2]

*Department of Biochemistry, Kanazawa Medical University School of Medicine, 1-1 Daigaku, Uchinada, Kahoku-gun, Ishikawa 920-0293, Japan, †Department of Nephrology, the First Hospital of China Medical University, Shenyang, People's Republic of China, and ‡Medical Research Institute, Kanazawa Medical University, 1-1 Daigaku, Uchinada, Kahoku-gun, Ishikawa 920-0293, Japan

sFlt-1 (soluble Flt-1) potently inhibits angiogenesis by binding extracellularly to VEGF (vascular endothelial growth factor). In the present paper, we report that hypoxia down-regulates sFlt-1 expression in HMVECs (human microvascular endothelial cells), a constituent of microvessels where angiogenesis occurs. Hypoxia (5–1 % O_2) increased VEGF expression in HMVECs. In contrast, the levels of sFlt-1 mRNA and protein in HMVECs decreased significantly as the O_2 concentration fell, whereas mFlt-1 (membrane-bound Flt-1) mRNA and protein remained unchanged. This suggested that hypoxia selectively regulates alternative 3′-end processing of sFlt-1 pre-mRNA. We have also demonstrated that sFlt-1 overexpression in lentiviral-construct-infected HMVECs counteracted VEGF-induced endothelial cell growth. We next identified *cis*-elements involved in sFlt-1 mRNA processing in HMVECs using a human Flt-1 minigene and found that two non-contiguous AUUAAA sequences function as the poly(A) signal. Furthermore, we identified a *cis*-element in intron 13 that regulates sFlt-1 mRNA processing. Mutagenesis of the U-rich region in intron 13 caused a significant decrease in the soluble-form/membrane-form RNA ratio in the minigene-transfected HMVECs. These results suggest that decreased sFlt-1 expression due to hypoxia contributes to hypoxia-induced angiogenesis and reveals a novel mechanism regulating angiogenesis by alternative mRNA 3′-end processing.

Key words: angiogenesis, hypoxia, mRNA 3′-end processing, soluble Flt-1, vascular endothelial cell, vascular endothelial growth factor (VEGF).

INTRODUCTION

Angiogenesis is the process by which new vascular networks are formed from pre-existing capillaries. This process is essential for embryogenesis, development and wound repair [1], and plays an important role in the progression of diseases such as cancers, diabetic retinopathy and rheumatoid arthritis [1]. A balance between endogenous positive and negative regulatory molecules strongly influences angiogenesis [2]. VEGF (vascular endothelial growth factor) is a central regulator of the angiogenic process in both physiological and pathological conditions [1]. VEGF stimulates proliferation and tube formation of vascular ECs (endothelial cells) by binding to specific cell-surface receptors. VEGF is expressed in ECs, a constituent of microvessels where angiogenesis occurs, and is up-regulated under hypoxia, which is the principal inducer of angiogenesis [3,4]. In addition, ECs express several angiostatic factors such as sFlt-1 (soluble Flt-1)/sVEGFR-1 [soluble VEGFR (VEGF receptor)-1], soluble neuropilin-1, thrombospondin and endostatin [5,6]. These results suggest that MVECs (microvascular ECs) employ both autocrine and paracrine loops which co-express VEGF and its antagonists to regulate angiogenesis.

sFlt-1, a potent anti-angiogenic factor, is produced by the gene encoding cell-surface mFlt-1 (membrane-bound Flt-1) by mRNA alternative 3′-end processing. sFlt-1 is composed of the extracellular domain of mFlt-1 and is capable of trapping its ligand VEGF. VEGF binds to Flt-1 with a much greater affinity (dissociation constant, approximately 2–10 pM) than that for KDR (kinase insert domain-containing receptor; also referred to as VEGFR-2), which is the major functional receptor for VEGF [7,8]. sFlt-1 regulates various physiological processes in tissues. For example, sFlt-1 expression maintains corneal avascularity [9], and spatially regulated sFlt-1 expression guides vessel sprouting and morphogenesis in developing blood vessels [10]. Excess circulating sFlt-1 has been implicated in the aetiology of endothelial dysfunction, hypertension and proteinuria in pre-eclampsia [11], and sFlt-1 overexpression has been reported to inhibit tumour growth and angiogenesis [12].

Although VEGF is known to be up-regulated in various tissues and cell types under hypoxia [3,4,13], the mechanisms that

Abbreviations used: ARE, A + U-rich element; bFGF, basic fibroblast growth factor; CFIM25, 25-kDa subunit of the cleavage factor Im; CstF, cleavage stimulation factor; Cst F64, 64-kDa subunit of CstF; DMOG, dimethyloxaloylglycine; EC, endothelial cell; FBS, fetal bovine serum; HEK-293TN cell, HEK (human embryonic kidney)-293 cell expressing the large T-antigen of SV40 (simian virus 40) and the neomycin-resistance gene; HIF, hypoxia-inducible factor; hnRNP, heterogeneous nuclear ribonucleoprotein; HUVEC, human umbilical vein EC; KDR, kinase insert domain-containing receptor; mFlt-1, membrane-bound Flt-1; MVEC, microvascular EC; HMVEC, human MVEC; PHD, prolyl hydroxylase; RT, reverse transcription; sFlt-1, soluble Flt-1; VEGF, vascular endothelial growth factor; VEGFR, VEGF receptor; sVEGFR, soluble VEGFR.

[1] These authors contributed equally to this work.

[2] To whom correspondence should be addressed (email yonekura@kanazawa-med.ac.jp).

regulate sFlt-1 expression in microvessels under these conditions have not yet been fully clarified. Furthermore, the relevant findings available in this regard are conflicting [14–16].

In the present study, we have investigated the regulation of sFlt-1 expression under hypoxia in primary cultured HMVECs (human MVECs). We have found that hypoxia down-regulates sFlt-1 expression, but not mFlt-1 expression, by mechanisms that may involve alternative 3′-end processing of sFlt-1 mRNA. Furthermore, we have identified the *cis*-elements that regulate this process.

EXPERIMENTAL

Cells

HMVECs isolated from neonatal dermis (Cascade Biologics) were maintained in HuMedia-EB2 medium supplemented with 5 % (v/v) FBS (fetal bovine serum), 5 ng/ml bFGF (basic fibroblast growth factor), 10 μg/ml heparin, 10 ng/ml EGF (epidermal growth factor), 1 μg/ml hydrocortisone and 39.3 μg/ml dibutyryl cAMP, according to the manufacturer's instructions (Kurabo). Hypoxia and proliferation experiments employing HMVECs were performed using HuMedia-EB2 medium supplemented with 0.1 % FBS, 5 ng/ml bFGF and 10 μg/ml heparin (assay medium). Briefly, cells were incubated for 24 h in a CO_2/tri-gas incubator (Astec) containing a mixture of 5 % (v/v) CO_2 and 1–10 % (v/v) O_2 balanced with N_2. The cells were viable after 24 and 48 h of exposure to hypoxia and continued to proliferate. Recombinant human VEGF (BD Biosciences) or DMOG (dimethyloxaloylglycine; Sigma–Aldrich) were added to the culture medium at the indicated concentration. HEK-293TN cells [HEK (human embryonic kidney)-293 cells expressing the large T-antigen of SV40 (simian virus 40) and the neomycin-resistance gene] (System Biosciences) were maintained in DMEM (Dulbecco's modified Eagle's medium; Sigma–Aldrich) supplemented with 10 % (v/v) FBS, 100 units/ml penicillin and 100 μg/ml streptomycin.

RT (reverse transcription)–PCR

Total RNA was isolated from HMVECs using the RNeasy Mini Kit (Qiagen) and was subjected to RT–PCR using the SuperScript® III One-Step RT–PCR System with Platinum® Taq DNA Polymerase (Life Technologies). The oligodeoxyribonucleotide primers employed are listed in Supplementary Table S1 (at http://www.BiochemJ.org/bj/436/bj4360399add.htm). Amplification conditions were as follows: temperatures and time periods for melting, annealing and extension were 95 °C for 15 s, 60 °C for 30 s and 68 °C for 30 s respectively. The conditions (amounts of RNA templates and cycle numbers for amplification) used resulted in linear amplification kinetics [3,4]. An aliquot of each reaction mixture was electrophoresed on a 2 % (w/v) agarose gel and stained with ethidium bromide.

Real-time RT–PCR

Real-time RT–PCR was performed to determine relative mRNA levels using the StepOnePlus Real-Time System (Life Technologies). mFlt-1, VEGF and KDR mRNA levels were measured using TaqMan Gene Expression Assays (Hs00176573_m1 for mFlt-1, Hs00900055_m1 for VEGF and Hs00911700_m1 for KDR; Life Technologies) and the TaqMan® RNA-to-C_T™ 1-Step Kit (Life Technologies), according to the manufacturer's instructions. The sFlt-1 mRNA level was measured using gene-specific primers (5′-TTGGGACTGTGGGAAGAAAC-3′ and 5′-TTGGAGATCCGAGAGAAAACA-3′) and the One Step SYBR® PrimeScript® RT–PCR Kit (Takara). β-Actin (human ACTB endogenous control; Life Technologies) was used as the internal control. Gene expression levels were analysed by plotting five-point serial standard curves using total RNA from HMVECs cultured under normoxia.

Western blotting

HMVECs were cultured under hypoxia (1 or 2.5 % O_2) or normoxia in the assay medium. The cells were collected and lysed with loading buffer [17]. Samples were electrophoresed on a 5–20 % (w/v) polyacrylamide gradient gel (e-PAGEL; ATTO) and transferred on to an Immobilon-P (Millipore) membrane using the Trans-Blot SD Cell (Bio-Rad Laboratories). After treatment with Odyssey blocking buffer (LI-COR Biosciences) for 1 h at room temperature (25 °C), the membrane was incubated at room temperature for 1 h with a rabbit anti-Flt-1 antibody (Y103; Epitomics) and a mouse anti-β-actin monoclonal antibody (AC-74; Sigma–Aldrich). The membrane was then incubated at room temperature for 1 h with IRDye 800CW anti-(rabbit IgG) antibody and IRDye 680 anti-(mouse IgG) antibody (LI-COR Biosciences), and visualized using an Odyssey IR imaging system (LI-COR Biosciences).

ELISA

HMVECs were cultured under hypoxia (1 or 2.5 % O_2) or normoxia in the assay medium. Protease inhibitors (Complete Mini; Roche Diagnostics) were added to the conditioned medium and centrifuged at 10 000 ***g*** for 15 min at 4 °C. The supernatants were collected and assayed for sFlt-1 using the Quantikine Human Soluble VEGFR1/Flt-1 Immunoassay Kit (R&D Systems) with recombinant human sFlt-1 and polyclonal antibodies against human sFlt-1. HMVEC-conditioned medium and cell lysates were analysed for VEGF using the Quantikine Human VEGF Immunoassay Kit (R&D Systems) with recombinant human $VEGF_{165}$ and anti-VEGF polyclonal antibodies. For preparation of HMVEC cell lysates, cells in 75-cm^2 flasks were washed with PBS and removed with a scraper after the addition of 1 ml of lysis buffer [PBS containing 1 % (w/v) Nonidet P40 and protease inhibitors]. Suspensions were then sonicated and centrifuged at 10 000 ***g*** for 10 min at 4 °C, and the supernatants were used for analysis.

Construction of lentiviral vectors and transduction of HMVECs

Human sFlt-1 and hnRNP (heterogeneous nuclear ribonucleoprotein) D cDNAs were generated from HMVEC template RNAs using the primers listed in Supplementary Table S2 (at http://www.BiochemJ.org/bj/436/bj4360399add.htm) and the TaKaRa High Fidelity RNA PCR Kit; the 5′- and 3′-primers contained EcoRI and NotI sites respectively. The amplified cDNAs were digested with EcoRI and NotI and inserted into the pCDH-CMV-MCS-EF1-copGFP vector (System Biosciences) that had been digested using the same restriction enzymes. Recombinant plasmid DNAs were purified using the EndoFree Plasmid Maxi Kit (Qiagen) and were subjected to nucleotide sequencing to verify their authenticity. Pseudoviral particles were generated by co-transfecting the pCDH vector and pPACKH1 Packaging Plasmid Mix (System Biosciences) into HEK-293TN cells using Lipofectamine™ (Life Technologies) and Plus™ Reagent (Life Technologies). At 1 day prior to infection,

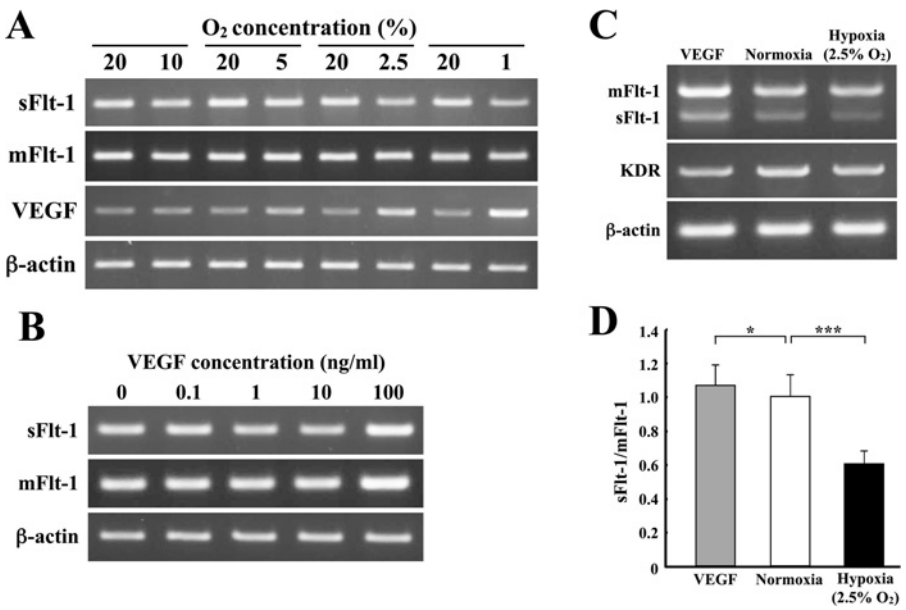

Figure 1 Hypoxia down-regulates sFlt-1 mRNA expression in HMVECs

(**A**) Expression of sFlt-1, mFlt-1, VEGF and β-actin mRNAs in HMVECs under normoxia or hypoxia. Total RNAs from HMVECs cultured for 24 h under the indicated oxygen tensions were analysed by RT–PCR using primers listed in Supplementary Table S1 (at http://www.BiochemJ.org/bj/436/bj4360399add.htm). An aliquot of each RT–PCR mixture was electrophoresed on a 2 % (w/v) agarose gel and visualized by ethidium bromide staining. (**B**) sFlt-1, mFlt-1 and β-actin mRNA expression in HMVECs in the presence of VEGF. Total RNAs from HMVECs cultured for 24 h in the presence of the indicated concentrations of VEGF were analysed by RT–PCR. (**C** and **D**) Determination of the sFlt-1/mFlt-1 mRNA ratio under hypoxia. (**C**) Total RNAs from HMVECs cultured under hypoxia (2.5 % O_2) or in the presence of 100 ng/ml VEGF were analysed by RT–PCR using the respective human-specific primers for sFlt-1 and mFlt-1 mRNAs in the same tube. KDR (VEGFR-2) and β-actin mRNA levels were also analysed by RT–PCR. (**D**) sFlt-1/mFlt-1 mRNA ratio. Quantification of the signal intensities of sFlt-1 and mFlt-1 mRNAs was performed using the public domain ImageJ program. Values are means $\pm$ S.D. ($n = 4$). Statistical significance was determined using a Student's t test for unpaired data. $^{*}P < 0.05$ and $^{***}P < 0.001$.

HMVECs were seeded at a density of $1–2 \times 10^5$ cells/well in a six-well plate and then infected with the lentiviral constructs in the presence of 5 μg/ml polybrene (Sigma–Aldrich). After 48 h, the expression of sFlt-1 and hnRNP D was determined by RT–PCR.

Cell proliferation assays

Lentiviral-construct-infected HMVECs were seeded at a density of 2×10^3 cells/well in a 96-well plate in 0.1 ml of assay medium. The cells were incubated for 24 h at 37 °C. Recombinant human VEGF (1 ng/ml) was then added and the cultures were incubated for another 3 days. After incubation, cell proliferation was evaluated by the cellular reduction of the tetrazolium salt WST-8 to formazan (Cell Counting Kit-8; Dojindo Laboratories).

Construction and expression of Flt-1 minigenes

An Flt-1 minigene (see Figure 6A) was constructed by inserting human Flt-1 gene fragments from exons 12 to 14, excluding the parts of introns 12 and 13 (nucleotide residues 98061–99023, 104664–106441 and 109486–110296 of GenBank® accession number NC_000013) into the pCI-neo mammalian expression vector (Promega). PCR-amplified fragments using the three primer pairs listed in Supplementary Table S2 were digested using the indicated restriction enzymes and inserted into the XhoI/NotI-digested pCI-neo vector. Sequence motifs for RNA-binding proteins in the Flt-1 minigene were searched using the 'Splicing Rainbow' at EBI database (http://www.ebi.ac.uk/asd-srv/wb.cgi?method=8), and mutations were generated using the GeneTailor Site-Directed Mutagenesis System (Life Technologies), according to the manufacturer's instructions, with the primers listed in Supplementary Table S1. Nucleotide sequencing verified that the mutations had been correctly introduced. HMVECs were transfected with these Flt-1 minigenes and the hnRNP D expression vector using jetPEI™-HUVEC (Polyplus Transfection). After 24 h, Flt-1 expression from the minigenes was determined by RT–PCR.

Statistical analysis

Statistical significance of the data was determined using a Student's t-test for unpaired data. Multiple comparisons were analysed by one-way ANOVA with Dunnett's and Bonferroni's post-hoc tests for significance using the Graphpad Prism 4 software. Statistical significance was defined as $^{*}P < 0.05$, $^{**}P < 0.01$ or $^{***}P < 0.001$.

RESULTS

Effect of hypoxia on sFlt-1 and mFlt-1 mRNA levels in HMVECs

RT–PCR analysis demonstrated that HMVECs expressed both sFlt-1 and mFlt-1 mRNAs (Figure 1). VEGF mRNA levels increased significantly as the O_2 concentration fell to 5 % and increased further at 2.5 and 1 % (Figure 1A). This result indicates that HMVECs were appropriately cultured under hypoxia [3,4]. In contrast, sFlt-1 mRNA levels decreased significantly as the O_2 concentration fell to 2.5 % and decreased further to 1 %, whereas mFlt-1 mRNA levels in HMVECs remained unchanged under hypoxia (Figure 1A). Since VEGF mRNA levels increased under hypoxia (Figure 1A), we examined the effects of VEGF on sFlt-1 and mFlt-1 mRNA levels (Figure 1B). Both sFlt-1 and mFlt-1 mRNA levels remained unchanged at low VEGF concentrations (0.1–10 ng/ml), but increased significantly at an

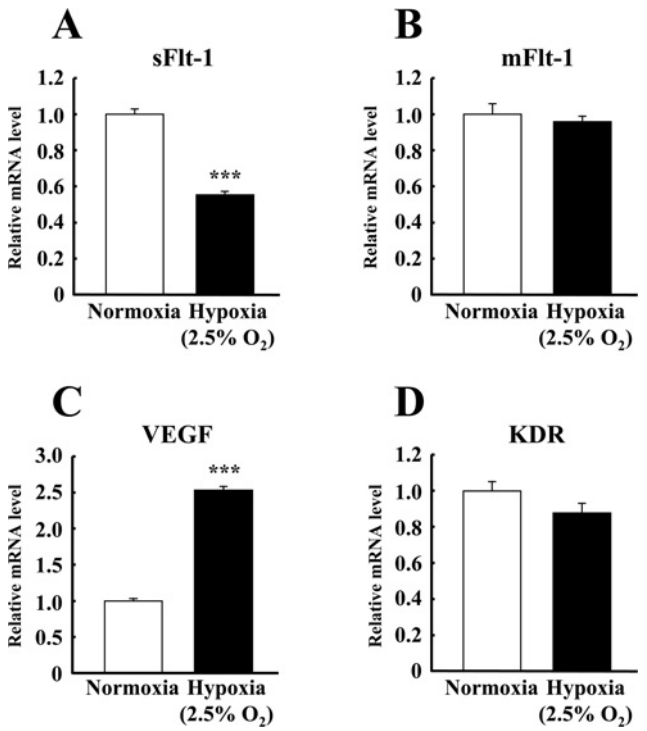

Figure 2 Real-time RT-PCR analysis of sFlt-1, mFlt-1, KDR and VEGF mRNAs in HMVECs under normoxia or hypoxia

Total RNAs were isolated from HMVECs cultured for 24 h under normoxia or hypoxia (2.5 % O_2). Relative sFlt-1 (**A**), mFlt-1 (**B**), VEGF (**C**) and KDR (**D**) mRNA levels were determined by real-time RT–PCR as described in the Experimental section. Values are means ± S.D. ($n = 3$). Statistical significance was determined using a Student's *t* test for unpaired data. ***$P < 0.001$.

extremely high VEGF concentration (100 ng/ml). We examined the VEGF protein levels in conditioned medium and HMVEC cell lysates that had been cultured under normoxia and hypoxia (1 and 2.5 % O_2) by ELISA. VEGF in cell lysates was undetectable under normoxia, and its protein levels increased to 27 and 31 pg/mg of protein under 2.5 % and 1 % O_2 respectively. VEGF in the conditioned medium was undetectable under all conditions. The VEGF levels were much lower than those that could affect Flt-1 expression. These results indicate that the hypoxia-induced increase in VEGF probably did not affect sFlt-1 mRNA levels.

We then determined relative sFlt-1 and mFlt-1 mRNA levels by simultaneous PCR-amplification using RNAs from HMVECs cultured under normoxia and hypoxia (2.5 % O_2) in the same tube using the primer pairs described in Supplementary Table S1 (Figure 1C). Densitometric analyses revealed that hypoxia caused significant decreases in the sFlt-1/mFlt-1 mRNA ratio, whereas the ratio remained unchanged or slightly increased in the presence of VEGF (Figure 1D). These results suggest that hypoxia regulates sFlt-1 mRNA levels at the level of alternative processing of its pre-mRNA. In comparison, KDR (VEGFR-2) mRNA levels remained unchanged under hypoxia (Figure 1C). We also determined relative sFlt-1, mFlt-1, KDR and VEGF mRNA levels by real-time PCR using the same RNAs described in Figure 1. As shown in Figure 2, the results were consistent with those obtained by RT–PCR (Figure 1).

To determine whether sFlt-1 mRNA and protein levels were co-ordinately expressed under normoxia and hypoxia (2.5 % O_2), we determined sFlt-1 protein levels secreted in the culture medium by ELISA (Figure 3A). sFlt-1 mRNA levels decreased to approximately 60 % under hypoxia (Figures 1D and 2A), and

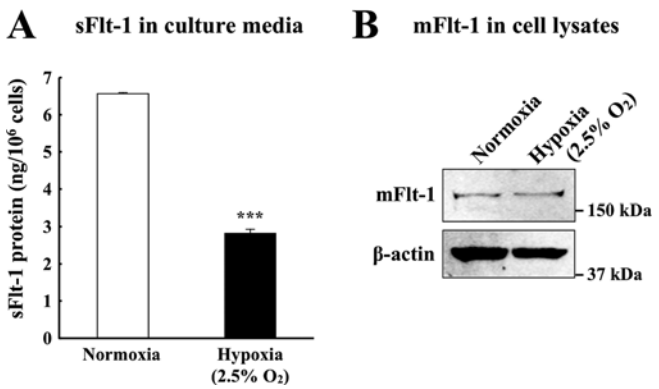

Figure 3 sFlt-1 and mFlt-1 protein levels under hypoxia

(**A**) Conditioned medium was collected from cells cultured for 24 h under normoxia or hypoxia (2.5 % O_2) and sFlt-1 protein levels were quantified by ELISA. Values are means ± S.D. ($n = 3$). Statistical significance was determined using a Student's *t* test for unpaired data. ***$P < 0.001$. (**B**) Western blot analysis of mFlt-1 protein in cell lysates prepared from HMVECs cultured as described in (**A**).

sFlt-1 protein levels (6.6 ng/10^6 cells, 3.4 ng/ml) also decreased to approximately 40 % (2.8 ng/10^6 cells, 1.2 ng/ml) under hypoxia (Figure 3A). mFlt-1 protein levels remained unchanged under hypoxia (Figure 3B) corresponding to mFlt-1 mRNA levels (Figures 1A and 2B).

Effect of DMOG on sFlt-1 and mFlt-1 mRNA levels in HMVECs

HIF (hypoxia-inducible factor)-1 plays a central role during the response to hypoxia [18]. Hypoxia stabilizes HIF-1α by inhibiting HIF-PHD (prolyl hydroxylase), which leads to HIF-1α degradation. Stabilized HIF-1α dimerizes with HIF-1β and activates the expression of multiple hypoxia-responsive genes, such as VEGF and erythropoietin.

To determine whether HIF-1 was involved in the decrease in sFlt-1 mRNA levels in hypoxic HMVECs, we examined the effect of a PHD inhibitor, DMOG [19], on Flt-1 expression. As shown in Figure 4, DMOG significantly increased VEGF mRNA levels in HMVECs, as observed under hypoxia, indicating that DMOG stabilized HIF-1α and enhanced HIF activity. The up-regulation of VEGF mRNA levels at DMOG concentrations of 50 and 100 μM (1.9- and 4.4-fold respectively; Figure 4E) was comparable with those under 2.5 and 1 % O_2 (Figures 1A and 2C). However, sFlt-1 and mFlt-1 mRNA levels increased with DMOG treatment (Figures 4C and 4D), but not under hypoxia (Figures 1A, 2A and 2B). The sFlt-1/mFlt-1 mRNA ratio at 50–100 μM DMOG remained unchanged (Figure 4B). These results indicate that HIF-1 was not directly involved in the hypoxia-induced decrease in sFlt-1 mRNA levels in HMVECs.

Effect of sFlt-1 overexpression on VEGF-induced HMVEC proliferation

Because sFlt-1 can trap VEGF in the extracellular space and thus inhibit EC growth [20], we next examined the effect of sFlt-1 overexpression on VEGF-induced HMVEC proliferation. Human sFlt-1 was overexpressed in HMVECs using a lentiviral vector, and the transduction efficiency was nearly 100 % according to GFP (green fluorescent protein) marker gene expression (results not shown). RT–PCR confirmed sFlt-1 overexpression in transduced HMVECs (Figure 5A). Transduced HMVECs were seeded on to a 96-well plate, incubated for 24 h and then

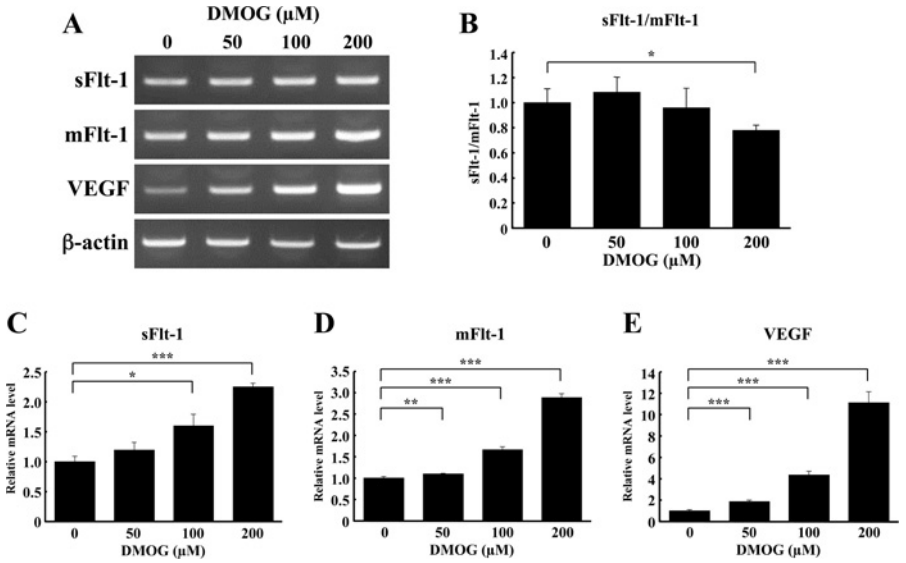

Figure 4 Effect of DMOG on Flt-1 expression in HMVECs

Total RNAs were isolated from HMVECs cultured for 24 h in the presence of the indicated concentration of DMOG. (**A**) RT–PCR analysis of mRNA levels for sFlt-1, mFlt-1 and VEGF. DMOG-treated HMVEC RNAs were analysed by RT–PCR using the primers listed in Supplementary Table S1 (at http://www.BiochemJ.org/bj/436/bj4360399add.htm). (**B**) Real-time RT–PCR analysis of mRNA levels to determine the sFlt-1/mFlt-1 ratio. Real-time RT-PCR analysis of sFlt-1 (**C**), mFlt-1 (**D**) and VEGF (**E**) mRNAs. Values are means ± S.D. ($n = 3$). Statistical significance was determined using a Student's *t*-test for unpaired data. $^{*}P < 0.05$, $^{**}P < 0.01$ and $^{***}P < 0.001$.

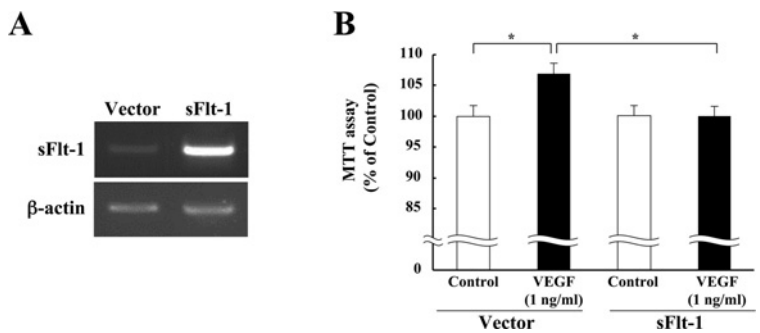

Figure 5 Effect of sFlt-1 overexpression on VEGF-induced HMVEC proliferation

(**A**) RT–PCR performed to determine sFlt-1 mRNA levels in HMVECs infected with a human sFlt-1 lentiviral construct. (**B**) Cell proliferation was evaluated as described in the Experimental section. Values are means ± S.E.M. ($n = 9$). $^{*}P < 0.05$. MTT, 3-(4,5-dimethylthiazol-2yl)-2,5-diphenyl-2*H*-tetrazolium bromide.

treated with recombinant human VEGF (1 ng/ml) for 3 days. After incubation, cell proliferation was assayed as described in the Experimental section. VEGF (1 ng/ml) moderately, but significantly, stimulated the proliferation of control (empty vector-transduced) HMVECs (107 %) (Figure 5B). However, VEGF failed to stimulate the proliferation of sFlt-1-overexpressing HMVECs (Figure 5B). These results indicate that sFlt-1 produced by HMVECs counteracted VEGF-induced EC proliferation in an autocrine manner.

The Flt-1 minigene mimics alternative Flt-1 mRNA 3′-end processing in HMVECs

To investigate *cis*-elements potentially regulating alternative processing of human Flt-1 pre-mRNA, we constructed a minigene that contains the Flt-1 sequences from exon 12 to exon 14, excluding segments of introns 12 and 13 (Figure 6A). We first identified nucleotide position 112 of intron 13 as the major processing site of sFlt-1 mRNA in HMVECs by 3′-rapid amplification of cDNA ends (results not shown); the result was consistent with that of a previous study using HUVECs (human umbilical vein ECs) [7]. The minigene included 1108 nucleotides of the 5′-region of intron 13 (Figure 6A). When the minigene was transfected into HMVECs, both soluble- and membrane-form RNAs were detected by RT–PCR (Figure 6B). The membrane form RNA generated by normal splicing and processing with the poly(A) signal in the vector was detected as an 850-bp band in the RT–PCR analysis. In contrast, the soluble-form RNA, which was cleaved and polyadenylated at the major processing site (nucleotide position 112 of intron 13), was detected as a 651-bp band. These results indicate that the minigene expressed both soluble- and membrane-form RNAs by a mechanism involving alternative mRNA processing.

Two non-contiguous AUUAAA sequences function as the poly(A) signal for sFlt-1 mRNA processing

The human Flt-1 gene contains two AUUAAA sequences just upstream of the major processing site of sFlt-1 mRNA (Figure 7A). To determine the sequences that function as the

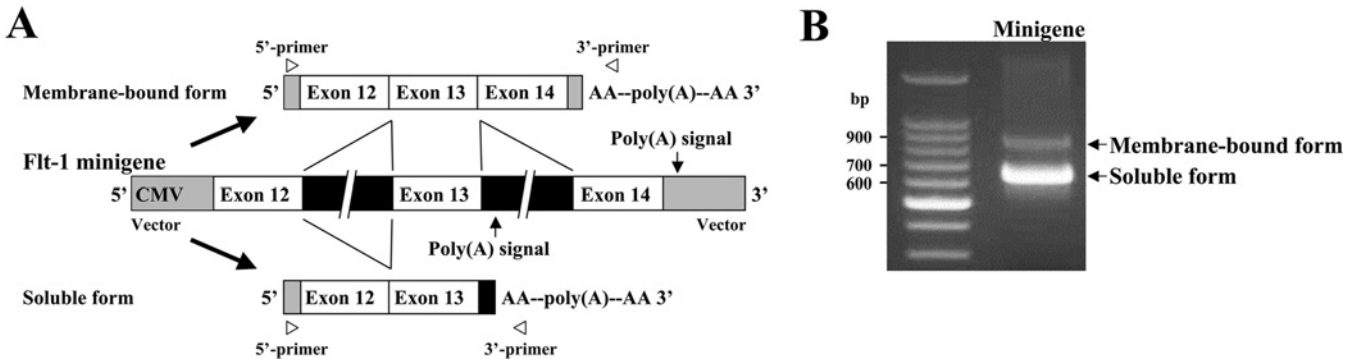

Figure 6 Human Flt-1 minigene construct and its products

(**A**) Schematic representation of the human Flt-1 minigene and its soluble- and membrane-form RNAs are displayed. The shaded boxes indicate the pCI-neo vector and the black boxes indicate the introns. The membrane-form RNA (top panel) was generated using the SV40 late poly(A) signal in the pCI-neo vector. The soluble form RNA (bottom panel) was generated using poly(A) signals in intron 13. Arrowheads indicate the 5′-primer (5′-TCCACTCCCAGTTCAATTACAG-3′) corresponding to vector sequences and the 3′-oligo d(T) anchor primer (5′-CTGATCTAGAGGTACCGGATCCTTTTTTTTTTTTTTTTV-3′). (**B**) RT–PCR simultaneously detected both membrane- (850 bp) and soluble- (651 bp) form RNAs.

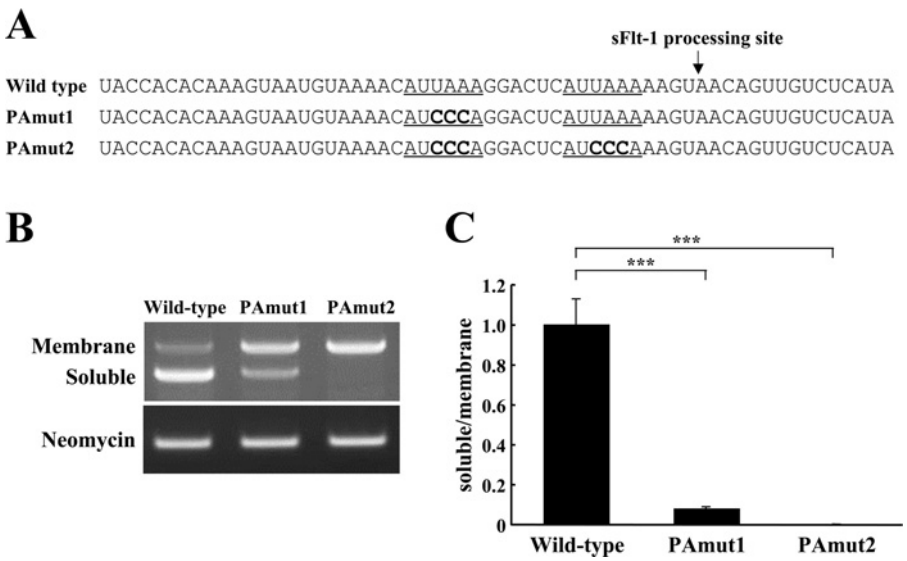

Figure 7 Mutational analyses of putative poly(A) signals for sFlt-1 mRNA

(**A**) The wild-type nucleotide sequence of a part of intron 13 of human Flt-1, which contains putative poly(A) signals, and those of mutations introduced into two non-contiguous AUUAAA sequences are shown. Putative poly(A) signals are underlined. Mutated nucleotides are in bold. The arrow indicates the major cleavage site of sFlt-1 mRNA. (**B**) Soluble- and membrane-form RNAs were detected by RT–PCR. Neomycin phosphotransferase (*neo*) mRNA expressed from the pCI-neo vector was used to normalize transfection efficiencies. (**C**) Soluble/membrane RNA ratio. Quantification of signal intensities was performed as described in the legend to Figure 1. The soluble/membrane RNA ratio for the wild-type minigene was assigned a value of 1. Values are means ± S.D. ($n = 3$). $^{***}P < 0.001$.

poly(A) signal, we introduced nucleotide substitutions at the putative poly(A) signals and examined the production of soluble-form RNA. Mutation of the upstream AUUAAA sequence (PAmut1) decreased soluble-form RNA levels to approximately 13 % and mutation of both AUUAAA sequences (PAmut2) decreased soluble-form RNA levels to nearly zero (Figure 7B). Transfection efficiencies were normalized using neomycin phosphotransferase (*neo*) mRNA, which was expressed from the minigene, as an internal control. When the soluble-form/membrane-form RNA ratio in the wild-type minigene was assigned the value of 1, the ratio in PAmut1 decreased to approximately 0.1 and decreased further to nearly zero in PAmut2 (Figure 7C). The results indicate that the upstream AUUAAA sequence plays a major role in sFlt-1 mRNA processing, and the downstream sequence was involved in cleavage and polyadenylation to some extent.

A U-rich region in Flt-1 intron 13 functions as a *cis*-element regulating sFlt-1 mRNA processing

To determine the potential regulatory elements controlling alternative processing of sFlt-1 pre-mRNA, we introduced a series of triplet nucleotide substitutions at putative recognition sequence motifs of RNA-binding proteins in exon and intron 13 of the Flt-1 minigene (Figure 8A, mut1–8). The sequences of five sites (mut1, mut2, mut4, mut7 and mut8) are putative serine/arginine splicing factor (SR) protein-binding motifs [21], and two (mut3 and mut6) are AREs (A + U-rich elements) specific for ARE-binding factors [22]. The mutation replacing UUU with AAA (mut6) dramatically decreased soluble-form RNA levels compared with those of the membrane form (Figure 8B), suggesting that the sequence was involved in the cleavage and polyadenylation of sFlt-1 mRNA. Another mutation (mut2) also decreased soluble-form RNA levels.

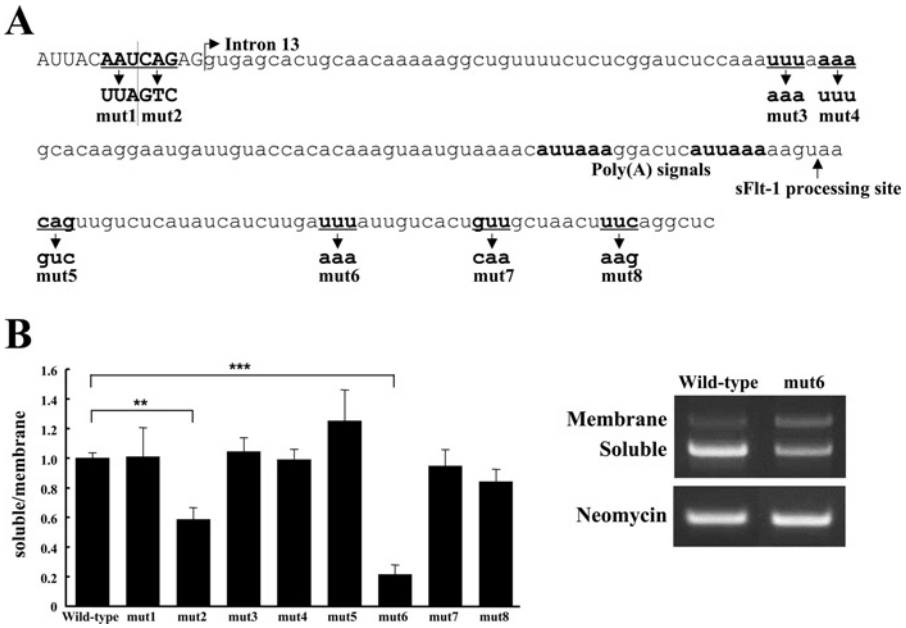

Figure 8 Effects of mutagenesis of intron 13 on alternative mRNA processing

(**A**) Nucleotide sequences of the end of exon 13 (uppercase letters) and the 5′-portion of intron 13 (lowercase letters) of the human Flt-1 gene, and mutations introduced into the minigene. Target nucleotides for the substitutions are in bold and underlined. (**B**) Soluble and membrane form RNAs were detected by RT–PCR. Quantification of signal intensities was performed as described in the legend to Figure 1. The soluble/membrane RNA ratio for the wild-type minigene was assigned a value of 1. Values are means ± S.D. ($n = 3$). RT–PCR results for control and mut6 minigene-transfected HMVECs are also shown. $^{**}P < 0.01$ and $^{***}P < 0.001$.

The position and sequence of the mut6 site, a U-rich element located 24 nucleotides downstream from the major cleavage site of sFlt-1 mRNA, suggested that the region is a possible binding site for CstF (cleavage stimulation factor) [23]. The significantly decreased production of soluble-form RNA by the mut6 minigene may be because of the elimination of CstF binding to intron 13 (Figure 8). CstF64 (64-kDa subunit of CstF) is essential for binding to the U-rich region, and up-regulation of CstF64 induces preferential utilization of an upstream poly(A) site [24,25]. In addition, Kubo et al. [26] have reported the involvement of CFIM25 (25-kDa subunit of the cleavage factor Im) in alternative poly(A)-site selection. However, both CstF64 and CFIM25 mRNA levels remained unchanged under hypoxia (10–1 % O_2) (results not shown). These results suggest that another mechanism might be involved in the regulation of hypoxia-induced alternative 3′-end processing of sFlt-1 mRNA.

hnRNP D overexpression affects alternative processing of sFlt-1 mRNA

The mut6 site is composed of a 5-nucleotide stretch, AUUUA. Similar sequences have been identified as binding sites for several RNA-binding proteins, including hnRNP A2/B1, HuR and hnRNP D [22]. To determine whether factors that bind to the mut6 site can affect the alternative processing of sFlt-1 mRNA, we examined the effects of hnRNP D (chosen as a model factor) overexpression because hnRNP D is known to bind to the AUUUA motif. A lentiviral vector carrying human hnRNP D cDNA was constructed, as described in the Experimental section, and was introduced into HMVECs. RT–PCR confirmed hnRNP D overexpression in transduced HMVECs (Figure 9A). Total RNAs were isolated from the control and transduced HMVECs, and endogenous sFlt-1 and mFlt-1 mRNA levels were examined by RT–PCR. As shown in Figure 9(A), hnRNP D overexpression significantly decreased sFlt-1 mRNA levels. Real-time PCR analysis confirmed the decrease in sFlt-1 mRNA levels in hnRNP D-overexpressing cells (Figure 9B).

Next, HMVECs were co-transfected with Flt-1 minigenes and hnRNP D, and soluble- and membrane-form RNA levels were evaluated by RT–PCR. As shown in Figures 9(C) and 9(D), hnRNP D overexpression decreased the soluble-/membrane-form RNA ratio to approximately 40 % in the wild-type and mut2 minigenes. hnRNP D overexpression also decreased the soluble-/membrane-form RNA ratio in the mut6 minigene (Figures 9C and 9D). The mut6 mutant still produced a small amount of soluble-form RNA (Figures 8B and 9C), suggesting that U-rich sequences around the original AUUUA site may serve as low-affinity CstF64-binding sites [23]. Therefore it is assumed that overexpressed hnRNP D competed with CstF64 in the 3′-end processing of sFlt-1 mRNA. These results suggest that competition between CstF and a factor that can bind to the mut6 site might possibly regulate alternative 3′-end processing of mRNA. However, it should be noted that mRNA levels of hnRNP A2/B1, HuR and hnRNP D remained unchanged under hypoxia (results not shown), suggesting that other factors or post-translational modifications of RNA-binding proteins might be involved in the regulation of this alternative processing.

DISCUSSION

In the present study, we have demonstrated that sFlt-1 expression in HMVECs, the constituent of microvessels where angiogenesis occurs, is down-regulated under hypoxia and this involves the alternative 3′-end processing of Flt-1 mRNA under these conditions.

Although sFlt-1 (sVEGFR-1) is suggested to be involved in both physiological and pathological angiogenesis [10–12,27], the mechanisms by which sFlt-1 expression is regulated have

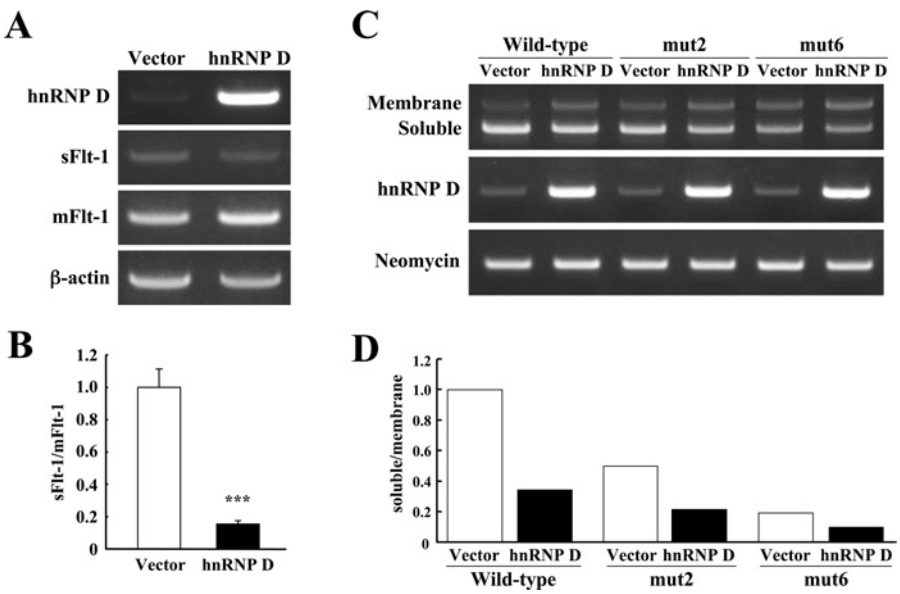

Figure 9 Effects of hnRNP D overexpression on alternative processing in HMVECs

(**A**) Effects of hnRNP D overexpression on alternative processing of endogenous sFlt-1 mRNA. Total RNAs from HMVECs transfected with control and human hnRNP D lentiviral constructs were analysed by RT–PCR with human-specific primers for sFlt-1 and mFlt-1 mRNAs. (**B**) The sFlt-1/mFlt-1 mRNA ratio. Relative mRNA levels were quantified by real-time RT–PCR using the same RNAs in (**A**), as described in the Experimental section. Values are means ± S.D. ($n = 3$). Statistical significance was determined using a Student's t test for unpaired data. $^{***}P < 0.001$. (**C**) Effects of hnRNP D overexpression on alternative processing of RNAs expressed by the Flt-1 minigene. Total RNAs from HMVECs co-transfected with the Flt-1 minigene and human hnRNP D were analysed by RT–PCR. (**D**) The soluble/membrane RNA ratio from (**C**). Quantification of the signal intensities of soluble-/membrane-form RNAs was performed using the ImageJ program.

not yet been fully clarified. Available results regarding sFlt-1 expression under hypoxia are conflicting. Xiong et al. [14] have reported that hypoxia leads to increased sFlt-1 secretion in HUVECs; however, other studies have demonstrated that sFlt-1 expression and secretion are not affected by hypoxia [15,16]. The discrepancy between the conclusions of previous studies and our present study may be due to the difference between microvasculature (HMVECs) and macrovasculature (HUVECs). mFlt-1 was reported to be up-regulated by hypoxia in HUVECs [28] and in MVECs derived from bovine corpus luteum and eyes [29,30]. A consensus binding site for HIF-1 is within the Flt-1 promoter [28]. In contrast, our present results show that mFlt-1 expression in HMVECs remains unchanged or is slightly decreased by hypoxia (Figures 1 and 2). In view of the marked decrease in sFlt-1 expression in HMVECs under hypoxia, we propose that sFlt-1 mRNA levels under these conditions are selectively regulated at the level of alternative 3′-end processing of its pre-mRNA.

HIF-1 plays a central role during the response to hypoxia [18]. We examined whether or not HIF-1 was involved in the hypoxia-induced decrease in sFlt-1 mRNA levels in HMVECs via the blockade of HIF-PHD that leads to HIF-1α degradation. In contrast with hypoxia, a PHD inhibitor, DMOG, increased both sFlt-1 and mFlt-1 mRNA levels at 50–100 μM DMOG (equivalent to 1–2.5 % O_2), but the sFlt-1/mFlt-1 mRNA ratio remained unchanged (Figure 4). These results indicated that HIF-1 was not directly involved in the hypoxia-induced decrease in sFlt-1 mRNA in HMVECs. Factors other than HIF-1 (probably as yet unidentified hypoxia-regulated RNA-binding proteins) may be involved in the regulation of alternative Flt-1 mRNA 3′-end processing under hypoxia.

VEGF stimulates EC proliferation, migration and tube formation by binding to KDR (VEGFR-2) [31]. sFlt-1 has been reported to function as a decoy receptor for VEGF, which suppresses VEGF-induced signalling [7–10,12]. In the present study, we report that sFlt-1 when overexpressed in HMVECs attenuates VEGF-induced EC proliferation (Figure 5). These results suggest that the hypoxia-induced decrease in sFlt-1 production and the corresponding increase in VEGF expression in HMVECs play an active role in EC proliferation under hypoxia. Thus sFlt-1 may be an essential component involved in autocrine regulation of angiogenesis.

In the present study, we also found *cis*-regulatory elements involved in sFlt-1 mRNA processing in HMVECs. We identified a major processing site (nucleotide position 112 in intron 13) of sFlt-1 mRNA produced in HMVECs. Mutational analyses of an Flt-1 minigene construct revealed that two non-contiguous AUUAAA sequences act as the poly(A) signal (Figure 7) and that a U-rich region 24 nucleotides downstream of the major cleavage site is essential for the 3′-end processing of sFlt-1 mRNA (Figure 8). The position and sequence of the U-rich element suggest that the region is a possible binding site for CstF [23]. However, CstF64 and CFIM25 mRNA levels remained unchanged under hypoxia (results not shown). On the other hand, overexpression of hnRNP D, an RNA-binding protein that can bind to this U-rich sequence, significantly decreased endogenous sFlt-1 mRNA levels, as well as the soluble/membrane RNA ratio expressed from the minigene (Figure 9). This suggests that competition between CstF and RNA-binding proteins that can bind to the U-rich element might possibly regulate alternative 3′-end processing of sFlt-1 mRNA. However, mRNA levels of possible U-rich element-binding proteins examined to date (hnRNP A0, hnRNP A2/B1, HuR and hnRNP D) remained unchanged under hypoxia (results not shown). We performed DNA microarray analysis of gene expression in HMVECs cultured under hypoxia (1 and 2.5 % O_2) using an Affymetrix GeneChip® array, but were unable to detect any RNA-binding protein transcripts whose expression levels changed under these conditions (results not shown). These

results suggest that post-translational modifications of RNA-binding proteins might be involved in regulating Flt-1 mRNA processing.

Although more studies are needed to clarify the *trans*-regulatory factors functioning on the *cis*-elements identified and their regulation under hypoxia, the results of the present study have revealed new aspects of sFlt-1 expression and function. We believe that our present study will provide new clues for clarifying further the mechanisms involved in regulating angiogenesis and for developing novel anti-angiogenesis therapeutic strategies for treating cancer and other angiogenesis-related diseases.

AUTHOR CONTRIBUTION

Takayuki Ikeda, Li Sun and Hideto Yonekura conceived the study. Takayuki Ikeda performed most of the minigene and lentivirus experiments, with contributions from Naoki Tsuruoka, Yasuo Yoshitomi and Yasuhito Ishigaki in some experiments, and wrote the paper. Li Sun performed most of the hypoxia experiments, with contributions from Takayuki Ikeda, Yoshino Yoshitake and Hideto Yonekura in some experiments. Naoki Tsuruoka constructed the Flt-1 minigene and its mutants. Yasuhito Ishigaki performed the DNA microarray analysis. Hideto Yonekura supervised the study and co-wrote the paper. All authors edited the manuscript prior to submission.

FUNDING

This work was supported in part by a Grant-in-Aid for Scientific Research from the Japan Society for the Promotion of Sciences [grant number 20590290]; a Grant for Collaborative Research from Kanazawa Medical University [grant number C2007-1]; a Grant for Project Research from the High-Technology Center of Kanazawa Medical University [grant number H2009-10]; and a Grant for Promoted Research from Kanazawa Medical University [grant numbers S2006-7, S2007-10 and S2009-9].

REFERENCES

1 Griffioen, A. W. and Molema, G. (2000) Angiogenesis: potentials for pharmacologic intervention in the treatment of cancer, cardiovascular diseases, and chronic inflammation. Pharmacol. Rev. **52**, 237–268
2 Hanahan, D. and Folkman, J. (1996) Patterns and emerging mechanisms of the angiogenic switch during tumorigenesis. Cell **86**, 353–364
3 Nomura, M., Yamagishi, S., Harada, S., Hayashi, Y., Yamashima, T., Yamashita, J. and Yamamoto, H. (1995) Possible participation of autocrine and paracrine vascular endothelial growth factors in hypoxia-induced proliferation of endothelial cells and pericytes. J. Biol. Chem. **270**, 28316–28324
4 Yonekura, H., Sakurai, S., Liu, X., Migita, H., Wang, H., Yamagishi, S., Nomura, M., Abedin, M. J., Unoki, H., Yamamoto, Y. and Yamamoto, H. (1999) Placenta growth factor and vascular endothelial growth factor B and C expression in microvascular endothelial cells and pericytes. Implication in autocrine and paracrine regulation of angiogenesis. J. Biol. Chem. **274**, 35172–35178
5 Wu, P., Yonekura, H., Li, H., Nozaki, I., Tomono, Y., Naito, I., Ninomiya, Y. and Yamamoto, H. (2001) Hypoxia down-regulates endostatin production by human microvascular endothelial cells and pericytes. Biochem. Biophys. Res. Commun. **288**, 1149–1154
6 Li, H., Yonekura, H., Kim, C. H., Sakurai, S., Yamamoto, Y., Takiya, T., Futo, S., Watanabe, T. and Yamamoto, H. (2004) Possible participation of *pICln* in the regulation of angiogenesis through alternative splicing of vascular endothelial growth factor receptor mRNAs. Endothelium **11**, 293–300
7 Kendall, R. L. and Thomas, K. A. (1993) inhibition of vascular endothelial cell growth factor activity by an endogenously encoded soluble receptor. Proc. Natl. Acad. Sci. U.S.A. **90**, 10705–10709
8 Waltenberger, J., Welsh, L. C., Siegbahn, A., Shibuya, M. and Heldin, C. H. (1994) Different signal transduction properties of KDR and Flt1, two receptors for vascular endothelial growth factor. J. Biol. Chem. **269**, 26988–26995
9 Ambati, B. K., Nozaki, M., Singh, N., Takeda, A., Jani, P. D., Suthar, T., Albuquerque, R. J. C., Richter, E., Sakurai, E., Newcomb, M. T. et al. (2006) Corneal avascularity is due to soluble VEGF receptor-1. Nature **443**, 993–997
10 Chappell, J. C., Taylor, S. M., Ferrara, N. and Bautch, V. L. (2009) Local guidance of emerging vessel sprouts requires soluble Flt-1. Dev. Cell **17**, 377–386
11 Maynard, S. E., Min, J. Y., Merchan, J., Lim, K. H., Li, J., Mondal, S., Libermann, T. A., Morgan, J. P., Sellke, F. W., Stillman, I. E. et al. (2003) Excess placental soluble fms-like tyrosine kinase 1 (sFlt1) may contribute to endothelial dysfunction, hypertension, and proteinuria in preeclampsia. J. Clin. Invest. **111**, 649–658
12 Goldman, C. K., Kendall, R. L., Cabrera, G., Soroceanu, L., Heike, Y., Gillespie, G. Y., Siegal, G. P., Mao, X., Bett, A. J., Huckle, W. R. et al. (1998) Paracrine expression of a native soluble vascular endothelial growth factor receptor inhibits tumor growth, metastasis, and mortality rate. Proc. Natl. Acad. Sci. U.S.A. **95**, 8795–8800
13 Shweiki, D., Itin, A., Soffer, D. and Keshet, E. (1992) Vascular endothelial growth factor induced by hypoxia may mediate hypoxia-initiated angiogenesis. Nature **359**, 843–845
14 Xiong, Y., Liebermann, D. A., Tront, J. S., Holtzman, E. J., Huang, Y., Hoffman, B. and Geifman-Holtzman, O. (2009) Gadd45a stress signaling regulates sFlt-1 expression in preeclampsia. J. Cell. Physiol. **220**, 632–639
15 Nagamatsu, T., Fujii, T., Kusumi, M., Zou, L., Yamashita, T., Osuga, Y., Momoeda, M., Kozuma, S. and Taketani, Y. (2004) Cytotrophoblasts up-regulate soluble fms-like tyrosine kinase-1 expression under reduced oxygen: an implication for the placental vascular development and the pathophysiology of preeclampsia. Endocrinology **145**, 4838–4845
16 Munaut, C., Lorquet, S., Pequeux, C., Blacher, S., Berndt, S., Frankenne, F. and Foidart, J. M. (2008) Hypoxia is responsible for soluble vascular endothelial growth factor receptor-1 (VEGFR-1) but not for soluble endoglin induction in villous trophoblast. Hum. Reprod. **23**, 1407–1415
17 Laemmli, U. K. (1970) Cleavage of structural proteins during the assembly of the head of bacteriophage T4. Nature **227**, 680–685
18 Fong, G. H. (2008) Mechanisms of adaptive angiogenesis to tissue hypoxia. Angiogenesis **11**, 121–140
19 Jaakkola, P., Mole, D. R., Tian, Y. M., Wilson, M. I., Gielbert, J., Gaskell, S. J., von Kriegsheim, A., Hebestreit, H. F., Mukherji, M., Schofield, C. J. et al. (2001) Targeting of HIF-α to the von Hippel-Lindau ubiquitylation copmplex by O_2-regulated prolyl hydroxylation. Science **292**, 468–472
20 Roeckl, W., Hecht, D., Sztajer, H., Waltenberger, J., Yayon, A. and Weich, H. A. (1998) Differential binding characteristics and cellular inhibition by soluble VEGF receptor 1 and 2. Exp. Cell Res. **241**, 161–170
21 Bourgeois, C. F., Lejeune, F. and Stevenin, J. (2004) Broad specificity of SR (serine/arginine) proteins in the regulation of alternative splicing of pre-messenger RNA. Prog. Nucleic Acid Res. Mol. Biol. **78**, 37–88
22 Barreau, A., Paillard, L. and Osborne, H. B. (2005) AU-rich elements and associated factors: are there unifying principles? Nucleic Acids Res. **33**, 7138–7150
23 Mandel, C. R., Bai, Y. and Tong, L. (2008) Protein factors in pre-mRNA 3′-end processing. Cell. Mol. Life Sci. **65**, 1099–1122
24 Chennathukuzhi, V. M., Lefrancois, S., Morales, C. R., Syed, V. and Hecht, N. B. (2001) Elevated levels of the polyadenylation factor CstF 64 enhance formation of the 1kB testis brain RNA-binding protein (TB-RBP) mRNA in male germ cells. Mol. Reprod. Dev. **58**, 460–469
25 Shell, S. A., Hesse, C., Morris, Jr, S. M. and Milcarek, C. (2005) Elevated levels of the 64-kDa cleavage stimulatory factor (CstF-64) in lipopolysaccharide-stimulated macrophages influence gene expression and induce alternative poly(A) site selection. J. Biol. Chem. **280**, 39950–39961
26 Kubo, T., Wada, T., Yamaguchi, Y., Shimizu, A. and Handa, H. (2006) Knock-down of 25 kDa subunit of cleavage factor Im in Hela cells alters alternative polyadenylation within 3′-UTRs. Nucleic Acids Res. **34**, 6264–6271
27 Wu, F. T. H., Stefanini, M. O., Gabhann, F. M., Kontos, C. D., Annex, B. H. and Popel, A. S. (2010) A systems biology perspective on sVEGFR1: its biological function, pathogenic role and therapeutic use. J. Cell. Mol. Med. **14**, 528–552
28 Gerger, H. P., Condorelli, F., Park, J. and Ferrara, N. (1997) Differential transcriptional regulation of the two vascular endothelial growth factor receptor genes. J. Biol. Chem. **272**, 23659–23667
29 Tscheudschilsuren, G., Aust, G., Nieber, K., Schilling, N. and Spanel-Borowski, K. (2002) Microvascular endothelial cells differ in basal and hypoxia-regulated expression of angiogenic factors and their receptors. Microvasc. Res. **63**, 243–251
30 Brylla, E., Tscheudschilsuren, G., Santos, A. N., Nieber, K., Borowski, K. S. and Aust, G. (2003) Differences between retinal and choroidal microvascular endothelial cells (MVECs) under normal and hypoxia conditions. Exp. Eye Res. **77**, 527–535
31 Olsson, A. K., Dimberg, A., Kreuger, J. and Claesson-Welsh, L. (2006) VEGF receptor signalling: in control of vascular function. Nat. Rev. Mol. Cell Biol. **7**, 359–371

Received 14 September 2010/16 February 2011; accepted 7 March 2011
Published as BJ Immediate Publication 7 March 2011, doi:10.1042/BJ20101490

Biochem. J. (2011) **436**, 399–407 (Printed in Great Britain) doi:10.1042/BJ20101490

online data

SUPPLEMENTARY ONLINE DATA

Hypoxia down-regulates sFlt-1 (sVEGFR-1) expression in human microvascular endothelial cells by a mechanism involving mRNA alternative processing

Takayuki IKEDA*[1], Li SUN*†[1], Naoki TSURUOKA*, Yasuhito ISHIGAKI‡, Yasuo YOSHITOMI*, Yoshino YOSHITAKE* and Hideto YONEKURA*[2]

*Department of Biochemistry, Kanazawa Medical University School of Medicine, 1-1 Daigaku, Uchinada, Kahoku-gun, Ishikawa 920-0293, Japan, †Department of Nephrology, the First Hospital of China Medical University, Shenyang, People's Republic of China, and ‡Medical Research Institute, Kanazawa Medical University, 1-1 Daigaku, Uchinada, Kahoku-gun, Ishikawa 920-0293, Japan

Table S1 Sequences of primers used for RT–PCR and site-directed mutagenesis

(a) Primers for RT – PCR

Gene	Sequence	Product size
sFlt-1 (sVEGFR-1)	5′-ATGTGCCAAATGGGTTTCAT-3′ 5′-TTGGAGATCCGAGAGAAAACA-3′	352 bp
mFlt-1 (mVEGFR-1)	5′-ATGCCACCTCCATGTTTGAT-3′ 5′-TAGATGGGTGGGGTGGAGTA-3′	317 bp
VEGF (VEGF-A)	5′-GCCTCCGAAACCATGAACTTTCTGCTG-3′ 5′-TGGTGATGTTGGACTCCTCA-3′	322 bp
KDR (VEGFR-2)	5′-GTGGGCTGATGACCAAGAAG-3′ 5′-TCACAAGGGTATGGGTTTGTC-3′	517 bp
hnRNP D	5′-GATCCTAAAAGGGCCAAAGC-3′ 5′-CCACTGTTGCTGTTGCTGAT-3′	306 bp
β-Actin	5′-CATCGAGCACGGCATCGTC-3′ 5′-CTCTTCTCCAGGGAGGAGC-3′	506 bp
Neomycin	5′-AGACAATCGGCTGCTCTGAT-3′ 5′-ATACTTTCTCGGCAGGAGCA-3′	261 bp

(b) Primers for site-directed mutagenesis (mutated sites are underlined)

Primer name	Sequence
PAmut1	5′-CACAAAGTAATGTAAAACATCCCAGGACTCATT-3′ 5′-ATGTTTTACATTACTTTGTGTGGTACAATC-3′
PAmut2	5′-AGGACTCATCCCAAAGTAACAGTTGTCTCATAT-3′ 5′-ATGAGTCCTGGGATGTTTTACATTACTTTG-3′
mut1	5′-CTCCAGAAGAAAGAAATTACTTACAGAGGTGAG-3′ 5′-GTAATTTCTTTCTTCTGGAGGATTTCTTCC-3′
mut2	5′-AGAAGAAAGAAATTACAATGTCAGGTGAGCACT-3′ 5′-ATTGTAATTTCTTTCTTCTGGAGGATTTCT-3′
mut3	5′-TTTTCTCTCGGATCTCCAAAAAAAAAAGCACAA-3′ 5′-TTTGGAGATCCGAGAGAAAACAGCCTTTTT-3′
mut4	5′-TCGGATCTCCAAATTTATTTGCACAAGGAATGA-3′ 5′-TAAATTTGGAGATCCGAGAGAAAACAGCCT-3′
mut5	5′-AAGGACTCATTAAAAAGTAAGTCTTGTCTCATA-3′ 5′-TTACTTTTTAATGAGTCCTTTAATGTTTTA-3′
mut6	5′-GTTGTCTCATATCATCTTGAAAAAATTGTCAATG-3′ 5′-TCAAGATGATATGAGACAACTGTTACTTTT-3′
mut7	5′-CATCTTGATTTATTGTCACTCAAGCTAACTTTC-3′ 5′-AGTGACAATAAATCAAGATGATATGAGACA-3′
mut8	5′-TGTCACTGTTGCTAACTAAGAGGCTCGGAGGAG-3′ 5′-AGTTAGCAACAGTGACAATAAATCAAGATG-3′

[1] These authors contributed equally to this work.
[2] To whom correspondence should be addressed (email yonekura@kanazawa-med.ac.jp).

Table S2 Sequences of primers used for cloning of Flt-1 and hnRNP D

Restriction enzyme sites are underlined.

Use of primer	Sequence	Restriction enzyme	Product size
sFlt-1 cDNA cloning	5′-GAGAATTCGAACGAGAGGACGGACT-3′	EcoRI	2157 bp
	5′-GAGCGGCCGCGAGTCCTTTAATGTTTTACATTAC-3′	NotI	
hnRNP D cloning	5′-CGAATTCGCCACCATGTCGGAGGAGCAGTTCGG-3′	EcoRI	893 bp
	5′-AGATCCTTGCGGCCGCTTAGTATGGTTTGTAGCTAT-3′	NotI	
Amplifying exon 12 and a part of intron 12 of Flt-1	5′-AGCTCGAGATGGCTAGCACCTTGGTTGTGGCTGAC-3′	XhoI	979 bp
	5′-GAACGCGTGATATCTCCCATGGCACAGA-3′	MluI	
Amplifying exon 13 and a part of intron 12 and 13 of Flt-1	5′-GAACGCGTTGAGATCATGCCACAGCACT-3′	MluI	1794 bp
	5′-GAGTCGACTGCATATGGGGAAAGTGGAC-3′	SalI	
Amplifying a part of intron 13 and exon 14 of Flt-1	5′-GAGTCGACTGTGCCTCTGCCTCTTGAAT-3′	SalI	777 bp
	5′-GAGCGGCCGCGGGGCTGATGAAAGATGAGA-3′	NotI	

Received 14 September 2010/16 February 2011; accepted 7 March 2011
Published as BJ Immediate Publication 7 March 2011, doi:10.1042/BJ20101490